Relationship between tree row LIDAR-volume and leaf area density for fruit orchards and vineyards obtained with a LIDAR 3D dynamic measurement system

R. Sanz [a,] *, J.R. Rosell [a] , J. Llorens [b] , E. Gil [b] , S. Planas [a]

[a] Department of Agro-forestry Engineering, University of Lleida, Avinguda Rovira Roure 191, 25198 Lleida, Spain
[b] Department of Agri Food Engineering and Biotechnology, Politechnical University of Catalunya, Campus del Baix Llobregat, edifici D4, Esteve Terrades, 8. 08860 Castelldefels, Spain

* Corresponding author. Tel.: +34 973 702863; fax: +34 973 702673.
E-mail address: rsanz@eagrof.udl.cat (R. Sanz).

Abstract

In this work, a LIDAR 3D Dynamic Measurement System, based on a Two-Dimensional Terrestrial Laser-LIDAR Scanner (2D TLS), was used for the geometric characterisation of tree-row crops (apple trees, pear trees and vineyards). The trees were scanned with the LIDAR system from opposite sides to obtain two three-dimensional point clouds. The point clouds were registered and the volume occupied by the resulting point cloud, tree row LIDAR-volume (TRLV), was graphically and numerically obtained. The study undertaken in this paper is based on the hypothesis that there may exist a non-linear relationship between the TRLV and the leaf area density (LAD). The main objective is to examine the relationship between TRLV and LAD in vineyards, apple and pear orchards. The study of 35 blocks of vegetation reveals a good logarithmic fit, $y= -0.36 \ln(x) + 3.69$ with $R^2=0.87$, between the TRLV (x) in dm^3 and the LAD (y) in dm^{-1}. It would appear that the TRLV of the crops under study (planted in a hedgerow-type configuration) is in itself an explanation of the LAD. The competition for light between the leaves and the space that these leaves occupy appear to follow a similar model in the three crops. According to the results of this study, the LAD can be estimated from the TRLV. If the LAD is multiplied by the TRLV, the leaf area of the vegetation under study can be obtained. It is therefore concluded that by using the information provided by the LIDAR 3D Dynamic Measurement System, a good estimation can be obtained of the leaf area in hedgerow fruit tree crops and hedgerow vineyards.

Keywords:
Terrestrial LIDAR scanners, 3D canopy structure, Tree volume, Leaf area density, Vineyard, Fruit tree

1. Introduction

The geometric characterisation of tree crops is a precision activity which entails accurate measurement and understanding of the geometry and structure of the many elements that make up the trees. One of the most important objectives of this activity is to ensure that the supply of crop inputs such as plant protection products (PPP), water, and fertilizer, etc., is appropriate to the local requirements of the crop or even to the individual requirements of each tree. Such precision results in economic savings, increased production, better quality and a reduction in environmental impact.

The main difficulty that arises when attempting to provide structural descriptions of trees lies in the complexity of the three-dimensional layout of the elements that comprise the trees. For this reason, parameters are commonly used which are the result of this vegetation structure. One of the most commonly studied parameters is the Leaf Area Index (LAI) (Zheng and Moskal, 2009). This is presently defined as half the leaf area per unit of ground surface (Chen and Black, 1992). The leaf area is an extremely important parameter because it is strongly related to processes such as evapotranspiration, radiation interception, and CO_2 fixation, etc. (Testi et al., 2004; Cohen et al., 2005; Williams and Ayars, 2005; Goodwin et al., 2006; Orgaz et al., 2006; Pereira et al., 2007; Pereira and Green, 2007; Lopez-Lozano et al., 2011)

The leaf area can be calculated by direct measurement which involves a lot of time and expense or it can be indirectly estimated using remote sensors and without any physical contact with the leaves (Zheng and Moskal, 2009; Rosell and Sanz, 2012). This can be achieved through a variety of detection approaches including, among others, image analysis techniques, digital stereoscopy photography, analysis of canopy light penetration, ultrasonic sensors and laser scanning techniques. From the perspective of the geometric characterisation of tree crops, Rosell and Sanz, (2012) undertook a comparison of all these techniques, analysing the physical principles, the most notable characteristics and the main advantages and disadvantages behind each technique.

One of the most promising technologies for the geometric characterisation of tree crops in the agricultural sphere is based on the use of LIDAR (Light Detection and Ranging) sensors (Dworak et al., 2011). The use of this type of sensor is based on the measurement of the distance from a laser emitter to an object or surface using a laser beam. Its principal characteristics include, most notably, a fast measuring speed and a high degree of precision. LIDAR systems can generate 3D digitalized images of crops with sufficient precision for most agriculture applications. A vast amount of information can be obtained from these images including height, width, volume, LAI and leaf area density (LAD) (Lee and Ehsani, 2009).

Two-Dimensional Terrestrial Laser-LIDAR Scanners (2D TLS) make two-dimensional sweeps in just one measuring plane. The additional third dimension can be obtained by moving the LIDAR in a perpendicular direction to the scanning plane. Though 2D TLS systems are normally simpler and more affordable than 3D TLS systems they tend to be less

accurate and it can be difficult to properly control the movement of the LIDAR when collecting the data.

Only a few studies have been carried out using TLS systems with tree crops. They have been classified into three groups. The first group includes two studies, which used data supplied by 3D TLS tripod-mounted systems (Moorthy et al., 2011; Keightley and Bawden, 2010). The second group covers various studies which used data obtained with 2D TLS tractor-mounted systems (Walklate, 1989; Walklate et al., 1997; Walklate et al., 2002; Wei and Salyani, 2004; Wei and Salyani, 2005; Lee and Ehsani, 2009; Palacín et al., 2007; Palleja et al., 2010; Llorens et al., 2011a). In this second group, the data obtained from the two sides of the fruit tree rows were not registered into a single system of coordinates. The third group of studies also used data obtained with tractor-mounted 2D TLS systems. However, in this group, the data acquired from the two sides of the fruit tree rows were registered into a single system of coordinates (Llorens et al., 2011b; Pascual et al., 2011; Sanz et al., 2011b; Rosell et al., 2009a,b). In brief, Llorens et al. (2011b) proposed a methodology to obtain a geo-referenced canopy density map by combining the information obtained with LIDAR with that generated using a global positioning system GPS receiver. This methodology was applied and tested on different vine varieties and crop stages, providing accurate information about the canopy distribution and/or location of damage along the rows. Pascual et al. (2011), in a four-year experiment on peach for fruit processing, evaluated canopy volume and tree shape by scanning trees with LIDAR. A relationship was obtained between the measured LIDAR tree volume and yield and fruit weight, suggesting that LIDAR offered a good way to evaluate fruit tree production capacity. The tree volume estimation system performed well when used as a component in the statistical analysis of the effects of irrigation strategy on productivity. Four papers have previously been published in relation to the work that is developed in the present paper. In Sanz et al. (2011a), an in-depth analysis was undertaken of the LIDAR sensor used (SICK-LMS200). The LIDAR-based 3D Dynamic Measurement System was presented and evaluated for the geometric characterisation of tree crops in Sanz et al. (2011b). A detailed explanation was provided in Rosell et al. (2009a,b) of the registration procedure of the point clouds, as well as the procedure used to obtain the tree row LIDAR-volume (TRLV). The initial relationships between leaf area, TRLV and manual-volume were also given. For reasons unrelated to the research process, the order in which these works were published does not necessarily reflect the order in which the studies were undertaken.

This introduction shows that the need to geometrically characterise tree crops can be satisfactorily met using TLS technology. The hypothesis and objectives of the present study will now be outlined.

1.4. Hypothesis and objectives

In this work, a LIDAR-based 3D Dynamic Measurement System was used for the geometric characterisation of tree-row crops. The trees were scanned with the LIDAR system from opposite sides to obtain two three-dimensional point clouds. The point clouds were registered and the volume occupied by the resulting point cloud was graphically and numerically obtained. Since the main function of plants is photosynthesis, the distribution

and position of the leaves is directly related to the availability of light. For this reason, the preferred position of leaves is normally in the outer part of the crown. Starting with these premises, this work is based on the hypothesis that there may exist a non-linear relationship between the TRLV and the LAD.

The specific objectives that are considered in this work are as follows:

- Study of the relationship between TRLV and LAD in apple tree orchards (*Malus communis* L. 'Red Chief' and 'Golden'), pear tree orchards (*Pyrus communis* L. 'Conference' and 'Blanquilla') and vineyards (*Vitis vinifera* L. 'Cabernet Sauvignon' and 'Merlot').
- Separate study, in apple and pear orchards and vineyards, of how the following variables affect the TRLV/LAD relationship: (i) the angular resolution of the LIDAR sensor, (ii) the height position of the LIDAR sensor and (iii) the length of the scanned vegetation (sample size).

2. Materials and methods

The measuring system employed in the present paper has been developed, tested and validated in studies undertaken by Rosell et al. (2009a,b) and Sanz-Cortiella et al. (2011a,b). The different components and operation of the system will therefore not be explained in detail in this section.

2.1. Location and main characteristics of the test orchards/vineyards

The orchards and vineyards used in the tests were arranged in rows of fruit trees and vines, forming continuous walls of vegetation (leaf walls). Table 1 contains data from the tests conducted in 2004. The various columns detail the crop species and variety, municipality, assigned block number, test date, block length in m, height in m of the vertical sections (strata) in ascending order and, in the final column, the LIDAR sensor height position from the ground in m. In all cases, the block length was equal to the distance between trunks. The leaf wall was divided into strata in order to study the distribution of the leaves by height.

Table 1
Tests conducted in 2004. Principal data.

Crop (village) / block	Test date	Block length (m)	Height of each strata (m)	LIDAR height position (m)
Pear *Conference* (Gimenells) / BI	20/05/04	1.5	0.4, 1, 1, 0.8	1.90
Pear *Conference* (Gimenells) / BII	16/07/04	1.5	0.4, 1, 1, 1	1.80
Pear *Blanquilla* (Gimenells) / BI	20/05/04	2.0	0.4, 1, 1, 1, 0.2	1.90
Pear *Blanquilla* (Gimenells) / BII	16/07/04	2.0	0.4, 1, 1, 0.7	1.90
Apple *Red Chief* (Gimenells) / BI	26/05/04	1.6	0.4, 1, 1, 1	1.80

Apple *Red Chief* (Gimenells) / BII	14/07/04	1.5	0.4, 1, 1, 1	1.80
Apple *Golden* (Gimenells) / BI	26/05/04	1.5	0.4, 1, 1, 1	1.90
Apple *Golden* (Gimenells) / BII	14/07/04	1.5	0.4, 1, 1, 1	1.90
Apple *Golden* (Lleida) / BI	30/05/04	1.2	0.4, 1, 1, 0.3	1.75
Apple *Golden* (Lleida) / BII	30/05/04	1.2	0.4, 1, 1, 0.4	1.80
Apple *Golden* (Lleida) / BIII	30/05/04	1.2	0.4, 1, 1, 0.4	1.80
Apple *Golden* (Lleida) / BIV	30/07/04	1.2	0.4, 1, 1, 0.7	1.80
Vineyard *Cabernet* (Caldes) / BI	03/06/04	2.0	0.3, 0.3, 0.3, 0.15	1.45
Vineyard *Cabernet* (Caldes) / BII	03/06/04	2.0	0.3, 0.3, 0.3, 0.3	1.45
Vineyard *Cabernet* (Caldes) / BIII	26/07/04	2.0	0.3, 0.3, 0.3, 0.3, 0.3	1.25
Vineyard *Merlot* (Caldes) / BI	03/06/04	2.0	0.3, 0.3, 0.3, 0.15	1.45
Vineyard *Merlot* (Caldes) / BII	03/06/04	2.0	0.3, 0.3, 0.3, 0.1	1.45
Vineyard *Merlot* (Caldes) / BIII	30/06/04	2.0	0.3, 0.3, 0.3, 0.3, 0.3	1.40
Vineyard *Merlot* (Caldes) / BIV	26/07/04	2.0	0.3, 0.3, 0.3, 0.3, 0.2	1.25

Table 2 contains data from the tests conducted in 2005. The various columns detail the crop species and variety, municipality, assigned block number, test date, block length in m and, in the final column, height in m of the vertical sections (strata) in ascending order. In the 2005 tests, four consecutive blocks of 1 m length were scanned and defoliated on each test date (Fig.1). This allowed the blocks to be grouped in pairs or in one group of four to facilitate a study of the effect of sample size on the results obtained. The nomenclature used is explained by way of the following examples. If two consecutive blocks BI_1 and BI_2 are put together, the resultant block is named BI_{12} with a length of 2 m. If the consecutive blocks BI_1 , BI_2 , BI_3 and BI_4 are combined, then the resultant block is named BI_{1234} with an overall length of 4 m. In all the 2005 tests the separation between trunks was 2 m. Unlike the 2004 tests, in 2005 there are two consecutive blocks – each 1 m long – between two trunks. The leaf wall is divided into strata in order to study the distribution of the leaves by height. In these tests the LIDAR sensor was placed in three different heights (Table 3).

Table 2

Tests conducted in 2005. Principal data.

Crop (village) / blocks	Test date	Block length (m)	Height of each strata (m)
Pear *Blanquilla* (Alfarrás) / BI_1, BI_2, BI_3, BI_4	18/04/05	1.0	0.2, 0.6, 0.6, 0.6, 0.6
Pear *Blanquilla* (Alfarrás) / BII_1, BII_2, BII_3, BII_4	03/05/05	1.0	0.2, 0.6, 0.6, 0.6, 0.6
Pear *Blanquilla* (Alfarrás) / $BIII_1$, $BIII_2$, $BIII_3$, $BIII_4$	02/06/05	1.0	0.2, 0.6, 0.6, 0.6, 0.6
Pear *Blanquilla* (Alfarrás) / BIV_1, BIV_2, BIV_3, BIV_4	25/07/05	1.0	0.2, 0.6, 0.6, 0.6, 0.6
Vineyard *Merlot* (Raimat) / BI_1, BI_2, BI_3, BI_4	10/05/05	1.0	0.2, 0.4, 0.3
Vineyard *Merlot* (Raimat) / BII_1, BII_2, BII_3, BII_4	06/06/05	1.0	0.35, 0.4, 0.4, 0.4
Vineyard *Merlot* (Raimat) / $BIII_1$, $BIII_2$, $BIII_3$, $BIII_4$	07/07/05	1.0	0.4, 0.4, 0.4, 0.4
Vineyard *Merlot* (Raimat) / BIV_1, BIV_2, BIV_3, BIV_4	24/08/05	1.0	0.4, 0.4, 0.4, 0.4

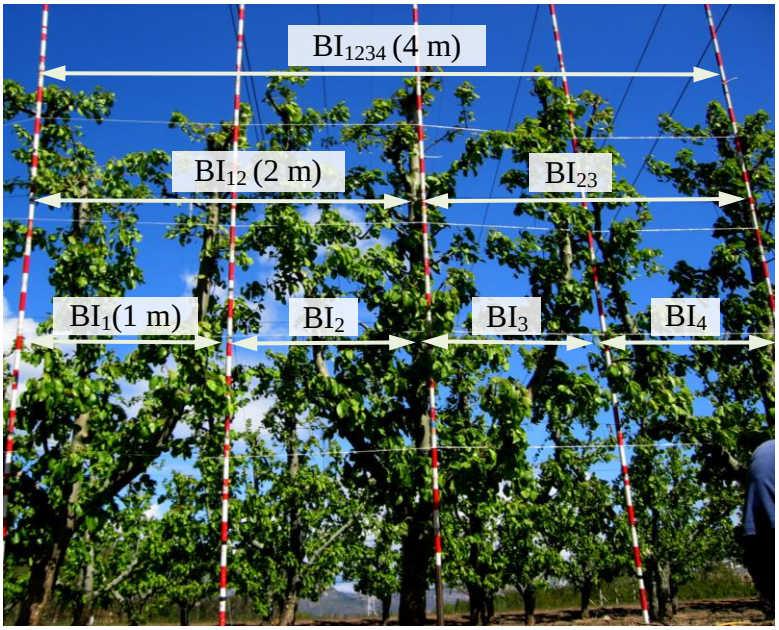

Fig. 1. Identification and grouping of blocks. Pear trees, 2005 (BI_1, BI_2, BI_3, BI_4, BI_{12}, BI_{23}, BI_{1234}). Test date 18/04/2005.

2.2. Description of the LIDAR sensor

The terrestrial Sick LMS200 LIDAR sensor was chosen for this study. This is a 2D TLS sensor which only scans in one measuring plane. This makes its cost very low compared to a 3D TLS. The latter generally makes more precise sweeps of three-dimensional spaces and with a greater distance range compared with the LMS200.

The LMS200 is an eye safe (Class 1), time-of-flight LIDAR sensor that emits at a wavelength of 905 nm (near infrared). Collaborative targets with specific reflectance features are not necessary and no lighting is required other than that provided by the emitted laser beam. The sensor gives the estimations in a polar form, providing a distance and its angle for each measuring point. Within the range from 0 to 8 m, the distance resolution is equal to 1 mm and the standard deviation is ±1.5 cm. The maximum angular range is 0°–180° but smaller ranges can be configured. In the field tests the beam directions of 0° and 180° were both vertical, pointing upwards and downwards, respectively. The angular resolution can be configured by the user with a choice of three possible values: 1°, 0.5° and 0.25°. The first two values were used in this test. The angular resolution of 0.25° was not used because the angular range is then limited to a maximum of 100°. Using the maximum angular range (0°–180°) and the selected angular resolution, the following information was obtained with each scan: (i) a total of 181 distance measurements using an angular resolution of 1°. These were obtained from a single complete rotation of the mirror. (ii) a total of 361 distance measurements using an angular resolution of 0.5°. These were obtained from two complete rotations of the mirror. Obtaining measurements with 0.5° angular resolution requires twice the amount of time compared with a 1° angular resolution. The number of measurements per second was the same with both angular resolutions. The

RS-232 data transfer protocol was used between the computer and the sensor at a speed of 38,400 bits per second. It was verified that at this communication speed the sensor performs 1,700 distance measurements per second. (Sanz et al., 2011b).

2.3. Measuring process and obtainment of TRLV

The LIDAR was used to obtain vertical slices of the tree surface. Each vertical slice was composed of the points of intersection between the laser beam and the vegetation. The scanning process involved the displacement of the measurement system along the left-hand and right-hand sides of the block under study (Fig. 2). The two scans were subsequently registered into a single point cloud. To ensure the correct registration of the two scans, in all tests, the tractor was displaced in a straight-line path at a constant speed between 1.0 and 2.1 km/h. Four reference planes were also used, two on each side, to facilitate the correct registration of the scans (Fig. 3). A detailed explanation was provided in Rosell et al. (2009b) of the registration procedure of the point clouds.

Fig. 2. LIDAR 3D Dynamic Measurement System (Rosell et al. 2009b; Sanz et al., 2011a,b; Rosell and Sanz 2012).

Fig. 3. Vineyard Merlot ($BIII_1$, $BIII_2$, $BIII_3$, $BIII_4$.) and reference planes.

After registration of the point clouds, the volume occupied by the resultant point cloud (TRLV) was graphically and numerically obtained.

The TRLV which the scanned vegetation occupies depends on: (i) the real size of the vegetation, (ii) the shape and size of the scan mesh and (iii) the position/s of the sensor with respect to the vegetation.

The mechanism used to obtain the TRLV was based on the intersection of two solids. The first solid was generated from the points obtained from the right-hand side of the scanned block (Fig. 4a). The end of the solid was located at more than 8 m from the sensor (maximum sensor distance range). This three-dimensional solid is equivalent to the shadow area which the laser emission of the LIDAR generates. The second solid was obtained in the same way as the first, this time using the points obtained from the left-hand side of the scanned block (Fig. 4b). The intersection of these two solids (Figs. 4c and 5a) gives us the TRLV (Rosell et al., 2009a). All the sensor generated points were used to obtain this volume, including both those that strike the vegetation as well as those that pass through the gaps. Data about the gaps is vital in order to obtain a better representation of the vegetation.

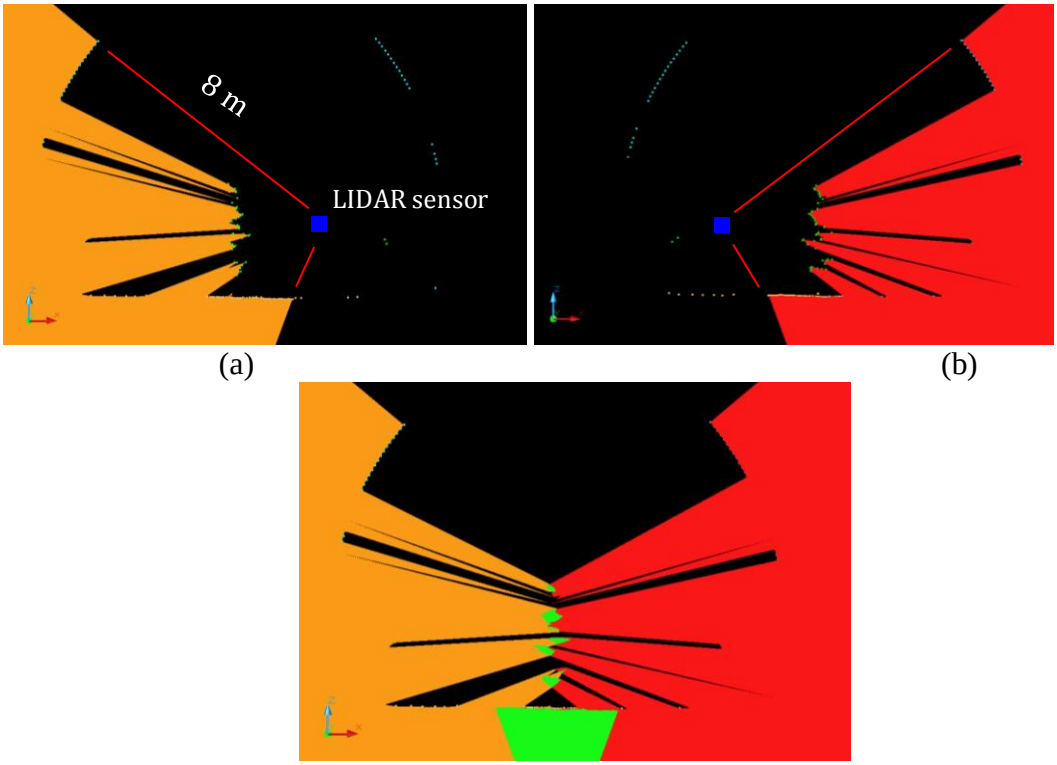

Fig. 4. Side views of the solids generated from the scanning of a very short section of vegetation, just 0.05 m long. (a) Solid obtained from the points generated after right-hand side scanning. (b) Solid obtained from the points generated after left-hand side scanning. (c) Result of the intersection (in green) of the (a) and (b) solids.

The procedure used in obtaining the TRLV is shown in Fig. 4. This example is based on the points scanned from both sides of a very short section of vegetation, just 0.05 m long. An isometric view of the solid obtained in Fig. 4c is shown in Fig. 5a, while Fig. 5b shows an isometric view of the TRLV obtained from a 2 m long section of vegetation.

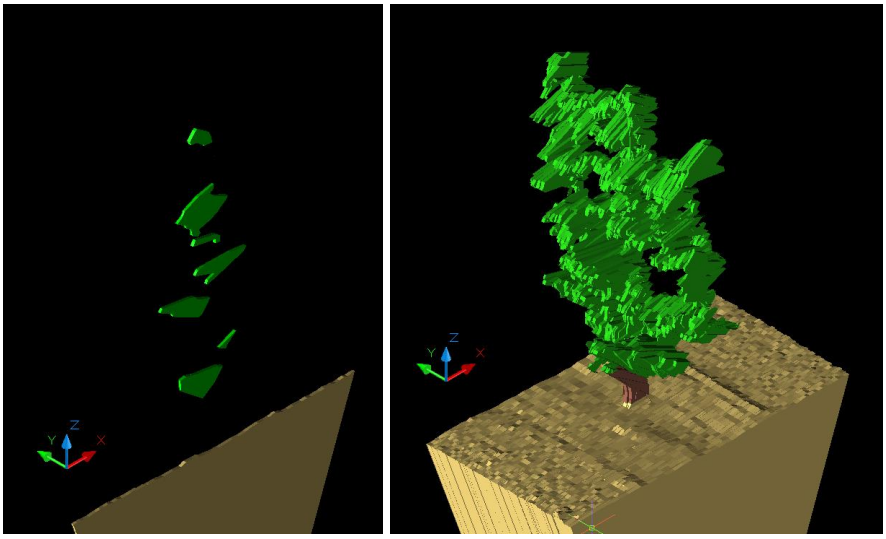

(a) (b)

Fig. 5. (a) Isometric view of the solid generated in Fig. 4c. (b) Isometric view of the TRLV of a 2 m long section of vegetation

2.4. Field test set-up

In the 2004 tests the distance between the sensor and the ground was the distance that allowed the sensor to be at half the height of the tree row (Table 1). The angular resolution of the sensor was always 1° and the scanned vegetation blocks were always between two trunks (Table 3).

In the 2005 tests new variables were incorporated in order to analyse their influence on the obtained TRLV. Three different height positions were used: an intermediate, upper and lower height. Two angular resolutions were used (1° and 0.5°). The results for the 4 consecutive 1 m long blocks were analysed as: (i) 4 independent blocks, (ii) 2 blocks of 2 m length and (iii) 1 block of 4 m length. The grouping enabled an analysis of the influence of the sample size (Table 3).

Table 3
Field test set-up.

Crop	Angular resolution	LIDAR height position (m)	Block length (m)
Apple, pear, vineyard (2004)	1°	Half the height of vegetation	Length between two trunks
Pear (2005)	1°, 0.5°	0.9, 2.1, 3.3	1, 2, 4
Vineyard (2005)	1°, 0.5°	1.2, 1.6, 2.0	1, 2, 4

Once the full canopy scan was done using LIDAR, all the leaves were then removed manually from each section to find the relationship between the LAD and the TRLV (Fig. 6). The planimeter used for this purpose was an Area Measurement System-Conveyor Belt Unit (Delta-T Devices Ltd.).

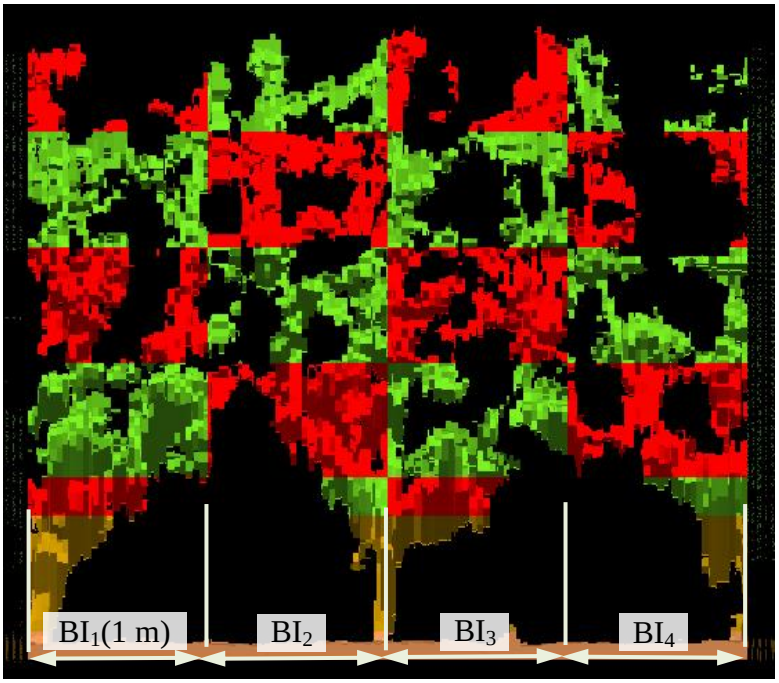

Fig. 6. Pear trees, 2005 (BI_1, BI_2, BI_3, BI_4). The TRLV which were to be related to the leaf area are shown in green and red. The lower leafless area was ignored and is shown in brown. The brown volume comprises the trunks and shadows generated by the upper leaves as a result of the position of the LIDAR.

3. Results and discussion

This section contains the results of the tests conducted during 2004 and 2005. Section 3.1 shows the overall results for 2004 and 2005 including all the crops used in the study. New variables were introduced in the design of the 2005 tests and, consequently, two new studies were undertaken, one on 'Blanquilla' pear trees (Section 3.2) and the other on 'Merlot' vines (Section 3.3). Though the actual studies undertaken were the same, the results will be presented separately since different crops were used.

3.1. Estimation of the LAD from the TRLV

In order to make it possible to compare the 2004 and the 2005 results, the only LIDAR data used in 2005 was the intermediate height position and 1° angular resolution.

Table 4 shows the following data and results for each defoliated block: year, crop, location, block identification, number of vertical divisions (strata), horizontal and vertical dimensions (H x V) of the scan mesh, TRLV, leaf area (S) and LAD (S/TRLV). The last two columns show the slope and coefficient of determination (R^2) of the regression line that passes through the point (0,0) between the leaf area and the TRLV of the sections that make up the block.

With regard to the scan mesh, the density and distribution of the impacts of the LIDAR sensor with the vegetation depends on the number of distances measured per second, the speed of advance of the system with respect to the vegetation, the selected angular resolution, the measured angular range and the distance between the sensor and the measured points. In Table 4, the Mesh column (H x V) is the theoretical grid in the frontal mid-plane of vegetation at the height of the LIDAR sensor. The forward speed during the measurement process was higher in the 2004 tests than in the 2005 tests. Also, the measured angular range was adjusted and therefore was made narrower in the 2005 tests than in the 2004 tests. These are the main reasons why the scan mesh (H x V) is smaller and therefore more precise in the 2005 tests.

Table 4
Data and results of the blocks studied.

Year / Crop (Village) / Block	No. strata	Mesh H x V (mm)	TRLV (dm^3)	S (dm^2)	LAD (S/TRLV) (dm^{-1})	Slope	R^2
2004 / Pear *Conference* (Gimenells) / BI	4	87 x 39	1333	1299	0.97	0.96	0.94
2004 / Pear *Conference* (Gimenells) / BII	4	60 x 39	1815	1372	0.76	0.73	0.98
2004 / Pear *Blanquilla* (Gimenells) / BI	5	89 x 40	3802	2367	0.62	0.59	0.89
2004 / Pear *Blanquilla* (Gimenells) / BII	4	65 x 36	3835	2461	0.64	0.68	0.96
2004 / Apple *Red Chief* (Gimenells) / BI	4	89 x 34	6399	2384	0.37	0.37	0.94
2004 / Apple *Red Chief* (Gimenells) / BII	4	56 x 35	6727	2770	0.41	0.41	0.86
2004 / Apple *Golden* (Gimenells) / BI	4	49 x 33	1797	1709	0.95	0.98	0.96
2004 / Apple *Golden* (Gimenells) / BII	4	62 x 41	1628	1554	0.95	0.95	0.97
2004 / Apple *Golden* (Lleida) / BI	4	49 x 39	2463	2149	0.87	0.88	0.97
2004 / Apple *Golden* (Lleida) / BII	4	51 x 40	2101	1929	0.92	0.95	0.98
2004 / Apple *Golden* (Lleida) / BIII	4	50 x 40	2495	1943	0.78	0.79	0.99
2004 / Apple *Golden* (Lleida) / BIV	4	27 x 39	2438	1980	0.81	0.83	0.98
2004 / Vineyard *Cabernet* (Caldes) / BI	4	48 x 30	126	205	1.62	1.42	0.84
2004 / Vineyard *Cabernet* (Caldes) / BII	4	50 x 29	135	263	1.94	1.62	0.68
2004 / Vineyard *Cabernet* (Caldes) / BIII	5	53 x 31	629	863	1.37	1.45	0.82
2004 / Vineyard *Merlot* (Caldes) / BI	4	49 x 31	102	186	1.82	1.80	0.98
2004 / Vineyard *Merlot* (Caldes) / BII	4	50 x 30	222	316	1.42	1.21	0.83
2004 / Vineyard *Merlot* (Caldes) / BIII	5	51 x 29	237	413	1.74	1.53	0.78
2004 / Vineyard *Merlot* (Caldes) / BIV	5	52 x 32	383	602	1.57	1.37	0.84
2005 / Pear *Blanquilla* (Alfarrás) / BI_{12}	5	20 x 40	595	937	1.57	1.58	0.94
2005 / Pear *Blanquilla* (Alfarrás) / BI_{34}	5	20 x 40	711	1050	1.48	1.40	0.93
2005 / Pear *Blanquilla* (Alfarrás) / BII_{12}	5	20 x 43	852	1425	1.67	1.60	0.92
2005 / Pear *Blanquilla* (Alfarrás) / BII_{34}	5	20 x 43	785	1201	1.53	1.47	0.95
2005 / Pear *Blanquilla* (Alfarrás) / $BIII_{12}$	5	18 x 41	1380	1842	1.33	1.26	0.92
2005 / Pear *Blanquilla* (Alfarrás) / $BIII_{34}$	5	18 x 41	1835	1906	1.04	1.03	0.94
2005 / Pear *Blanquilla* (Alfarrás) / BIV_{12}	5	18 x 43	1451	1541	1.06	1.08	0.98
2005 / Pear *Blanquilla* (Alfarrás) / BIV_{34}	5	18 x 43	1376	1537	1.12	1.10	0.89
2005 / Vineyard *Merlot* (Raimat) / BI_{12}	3	24 x 29	153	287	1.87	1.80	0.99

2005 / Vineyard *Merlot* (Raimat) / BI_{34}	3	22 x 31	176	317	1.79	1.75	0.98
2005 / Vineyard *Merlot* (Raimat) / BII_{12}	4	25 x 30	414	692	1.67	1.68	0.99
2005 / Vineyard *Merlot* (Raimat) / BII_{34}	4	23 x 29	441	766	1.74	1.70	0.99
2005 / Vineyard *Merlot* (Raimat) / $BIII_{12}$	4	24 x 29	705	1024	1.45	1.39	0.97
2005 / Vineyard *Merlot* (Raimat) / $BIII_{34}$	4	22 x 31	789	961	1.22	1.22	0.96
2005 / Vineyard *Merlot* (Raimat) / BIV_{12}	4	25 x 30	560	800	1.43	1.41	0.99
2005 / Vineyard *Merlot* (Raimat) / BIV_{34}	4	23 x 29	603	810	1.34	1.34	0.99

It can be seen in the final column of Table 4 that the R^2 values are very high. The R^2 of 26 of the 35 defoliated blocks was higher than 0.90, while it was below 0.80 in just two cases. The total number of defoliated sections was 150.

As the TRLV figures and their relationship to the defoliated leaf area were obtained, it was noted that the larger and more voluminous vegetation gave low LADs whereas the less voluminous vegetation had higher LADs. It can be seen from Table 4 that the low LADs (0.37 and 0.41 dm^{-1}) corresponded to the more voluminous trees, like the *Red Chief* apple variety. The highest LADs (1.22-1.94 dm^{-1}), on the other hand, corresponded to the vines, which are less voluminous. From this observation and following the initial hypothesis of this paper, a study was undertaken of the relationship between the TRLV and the LAD.

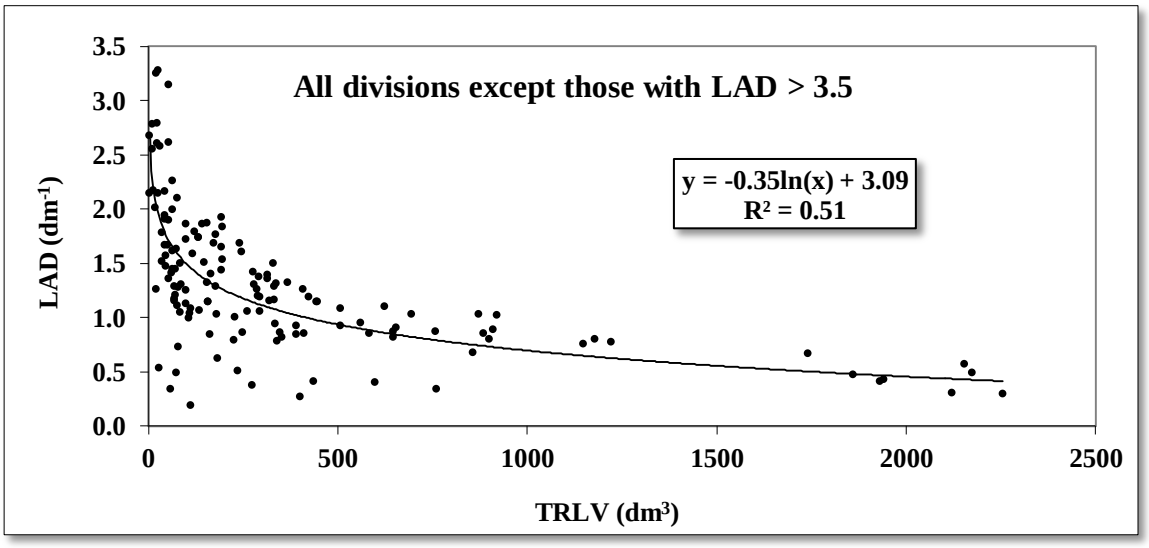

Fig. 7. Scatter diagram, logarithmic regression and R^2 of the relationship between the TRLV and LAD of all the defoliated sections except for the 6 sections with an LAD greater than 3.5 dm^{-1}.

Fig. 7 was generated with the TRLV and LAD results for each of the defoliated sections. The TRLV and LAD of all the sections are shown, except for the 6 sections with the highest LAD. These 6 values (6.2, 7.15, 9.6, 9.8, 11.0 and 37.7 dm^{-1}) correspond to the upper stratum of some defoliated vines in 2004, *Cabernet Sauvignon* and *Merlot*. The

TRLV of these sections are very small, lower than 4 dm^3, and are not representative of the vegetation. Discarding these points, an R^2 of 0.51 was obtained from the logarithmic fit.

After this initial result, the uppermost section of each of the blocks was discarded. The logarithmic fit which was then obtained, $y=-0.39\ln(x)+3.40$, gave an improved R^2 of 0.65 compared to the 0.51 of Fig. 7. The 6 sections discarded in Fig. 7 were part of the uppermost sections and were therefore also discarded in this case.

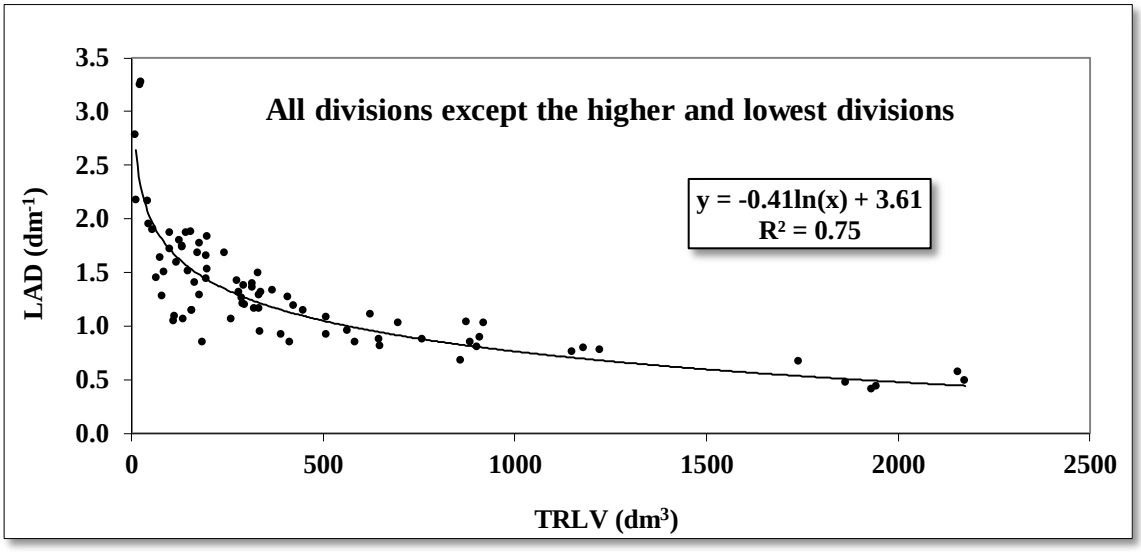

Fig. 8. Scatter diagram, logarithmic regression and R^2 of the relationship between the TRLV and the LAD of all defoliated sections, except for the 35 uppermost and the 35 lowermost sections.

Fig. 8 shows the result after discarding the uppermost and lowermost section of each block. The logarithmic fit thereby obtained gave an R^2 of 0.75, an improvement on the two previous cases (R^2=0.51, R^2=0.65). There is a clearly observable improvement in the R^2 as the upper and lower sections of the blocks are discarded. There is a possible twofold explanation for this: (i) the position of the sensor means that the uppermost and lowermost sections of the block are the furthest sections from the sensor and, therefore, are more likely to be hidden by the rest of the vegetation. In addition, the scanning angle does not facilitate the determination of the correct volume, with the tendency being to obtain higher volumes than there really are. (ii) The uppermost section is normally more irregular than the other sections, with less vegetation and more gaps.

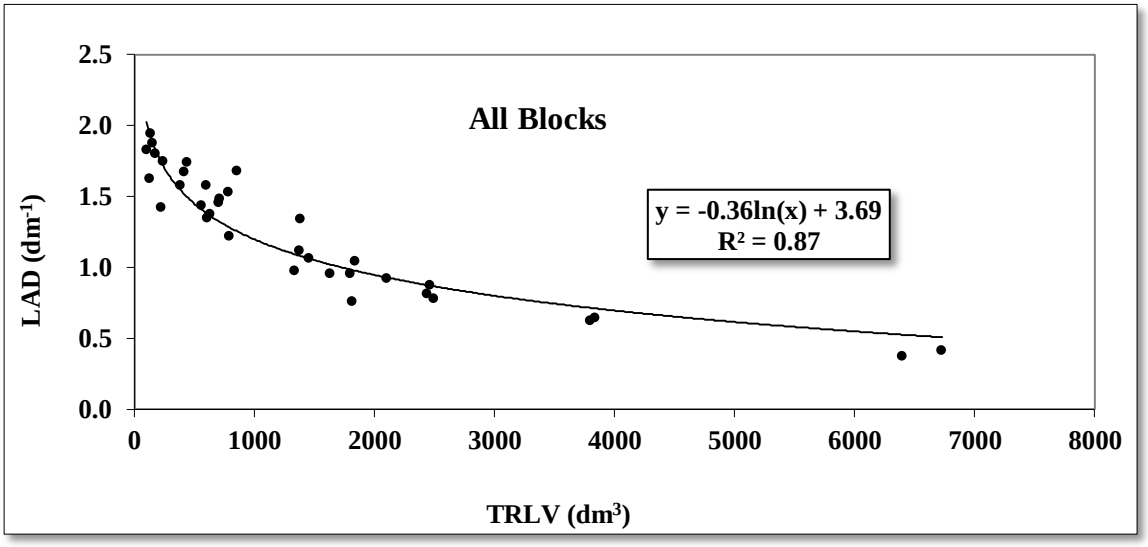

Fig. 9. Scatter diagram, logarithmic regression and R^2 of the relationship between the TRLV and the LAD of all 35 blocks, combining the sections of each block.

Fig.9 shows the result of the TRLV and LAD of the blocks, ignoring the internal divisions (sections). In this way each point represents the TRLV and LAD of the whole block. It can be seen that there is a very good logarithmic fit, with R^2=0.87. Grouping the sections together decreases the variability. The differential performance of the uppermost and lowermost sections of each block is smoothed out. It should be remembered that the size of the uppermost and lowermost sections was always equal to or less than the size of the central sections (Table 1, 2). This fact means that the weight of this differential performance in the block as a whole is less.

The relationship that was found confirms the starting hypothesis (the preferred position of leaves is normally in the outer part of the crown). It therefore makes sense that the LAD can be estimated from the TRLV (Eq.(1)).

Knowing that S = LAD×TRLV and stressing the fact that the preferred position of leaves is normally in the outer part of the crown, it also makes sense that S can be estimated from the TRLV (Eq. (2)):

$$LAD = -0.36 \times \ln(TRLV) + 3.69 \qquad (R^2 = 0.87) \tag{1}$$

$$S = (-0.36 \times \ln(TRLV) + 3.69) \times TRLV \tag{2}$$

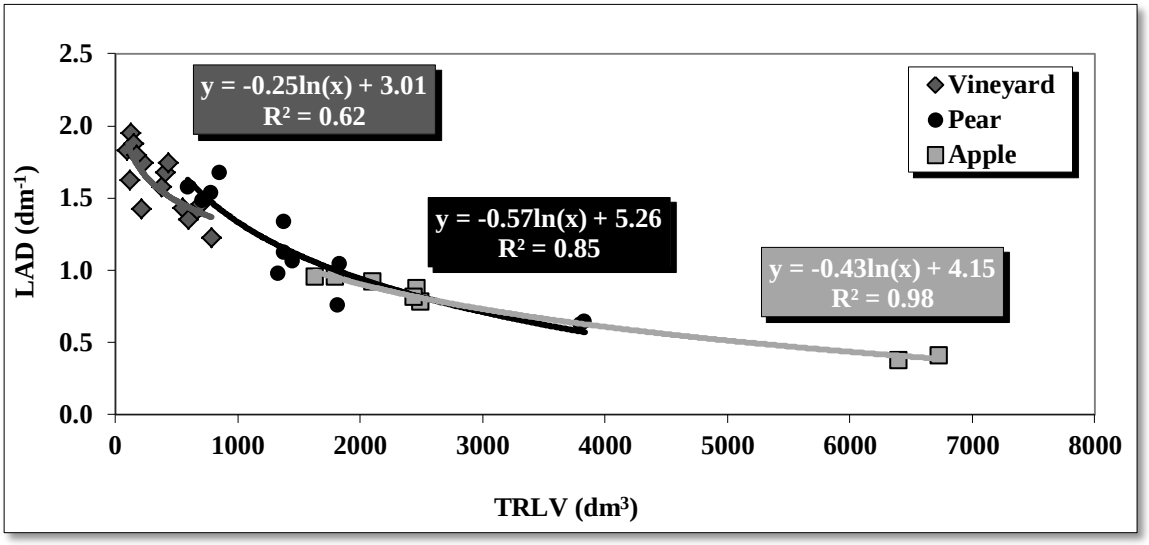

Fig. 10. Scatter diagram, logarithmic regression and R^2 of the relationship between the TRLV and the LAD for vine, pear and apple tree blocks, fitted independently.

Fig.10 is based on the same data used for Fig. 9, except that the vine, pear and apple tree blocks are independently fitted. The least favourable result was obtained for the vine blocks with R^2=0.62. This may be due to its geometric characteristics, namely its smaller size and greater degree of irregularity in comparison to the apple and pear blocks. The smaller and more irregular an object, the greater the precision required in its measurement. The fit obtained for the apple and pear trees was very good, with R^2=0.85 and R^2=0.98, respectively.

At plant level (block not subdivided into sections), and for the crops studied in this paper, the competition for light of the leaves and their occupation of space (volume) appears to follow a similar model.

A comparative study of the different species and locations of the vines, apples and pears is not feasible due to the relatively low amount of data available for each of them.

3.2. Specific study of the year 2005 in pear trees

The blocks used in this study did not take into account the sub-divisions into different strata. Separate analyses were conducted on the effects of the angular resolution and sensor position. It was firstly verified whether there was any significant difference when working with angular resolutions of 1° and 0.5°.

It can be observed in Fig. 11 that the curves of 1° and 0.5° are practically the same. As explained in Section 2.2, the number of measurements per second was the same with both angular resolutions. The difference between one and the other resolution lies in the distribution of the points in space. In the 0.5º resolution the separation between points of

the Y axis (travelling direction of the sensor) is twice that of the 1º resolution. However, twice the number of points are obtained in each vertical scan. In any case, it is shown in Fig. 11 that the different arrangement of the point mesh, in both resolutions, is not sufficient to generate significant differences in the measurement of the TRLV.

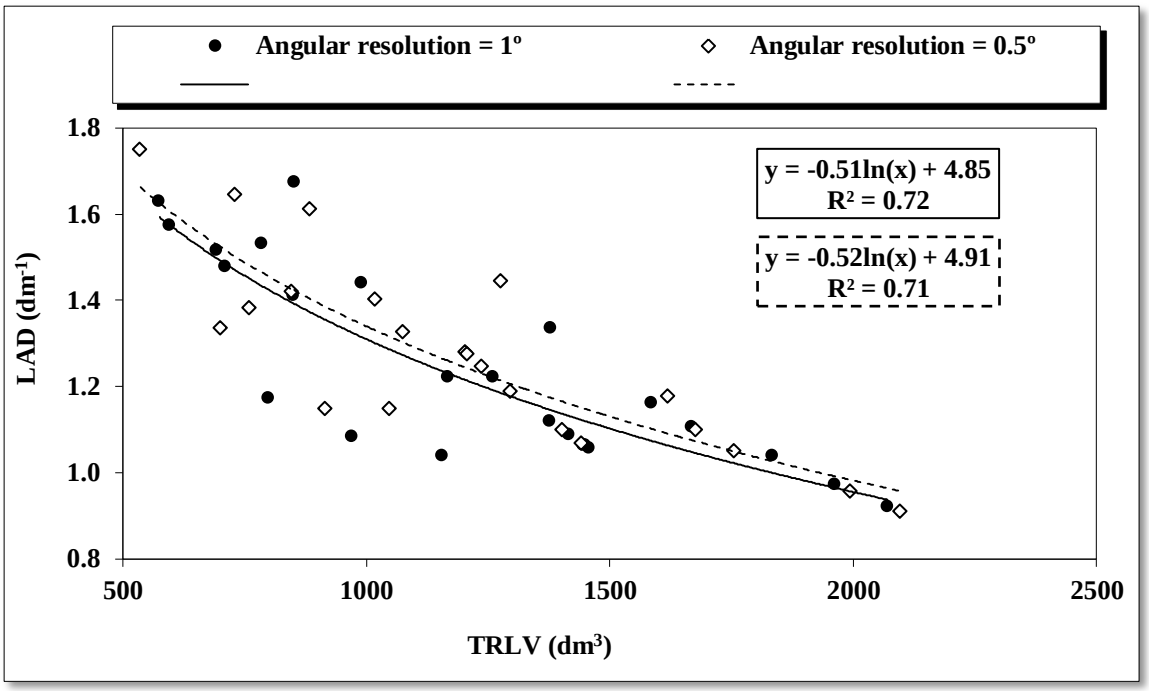

Fig. 11. Scatter diagram, logarithmic regression and R^2 of the relationship between TRLV and LAD of the 8 pear tree blocks, BI_{12}, BI_{34}, BII_{12}, BII_{34}, $BIII_{12}$, $BIII_{34}$, BIV_{12}, BIV_{34}. The TRLV were obtained from scans with the sensor placed at three different heights (0.9, 2.1 and 3.3 m) and two different angular resolutions (1° and 0.5°). The blocks scanned with an angular resolution of 1º are presented separately from those scanned with an angular resolution of 0.5º.

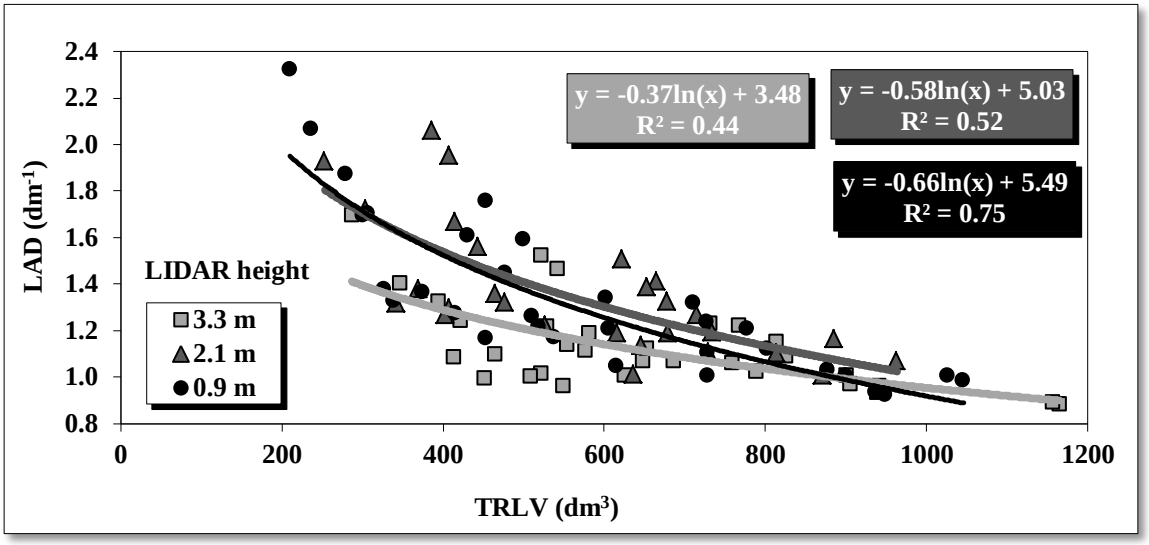
y = -0.37ln(x) + 3.48
R² = 0.44
y = -0.58ln(x) + 5.03
R² = 0.52
y = -0.66ln(x) + 5.49
R² = 0.75
LIDAR height
3.3 m
2.1 m
0.9 m
LAD (dm-1)
TRLV (dm3)
2.4
2.2
2.0
1.8
1.6
1.4
1.2
1.0
0.8
0
200
400
600
800
1000
1200

(a)

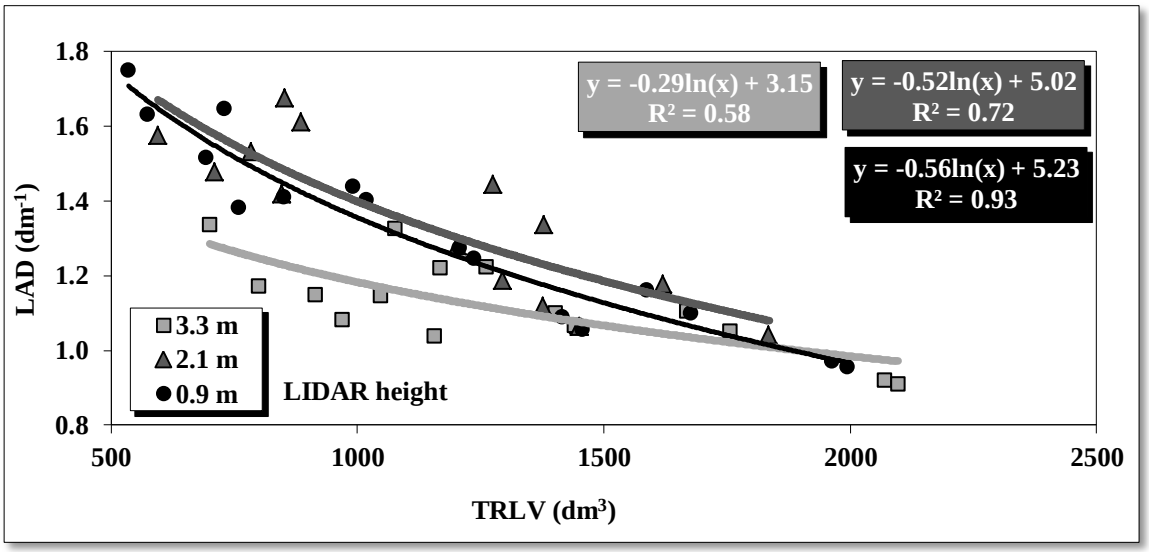
y = -0.29ln(x) + 3.15
R² = 0.58
y = -0.52ln(x) + 5.02
R² = 0.72
y = -0.56ln(x) + 5.23
R² = 0.93
3.3 m
2.1 m
0.9 m
LIDAR height
LAD (dm-1)
TRLV (dm3)
1.8
1.6
1.4
1.2
1.0
0.8
500
1000
1500
2000
2500

(b)

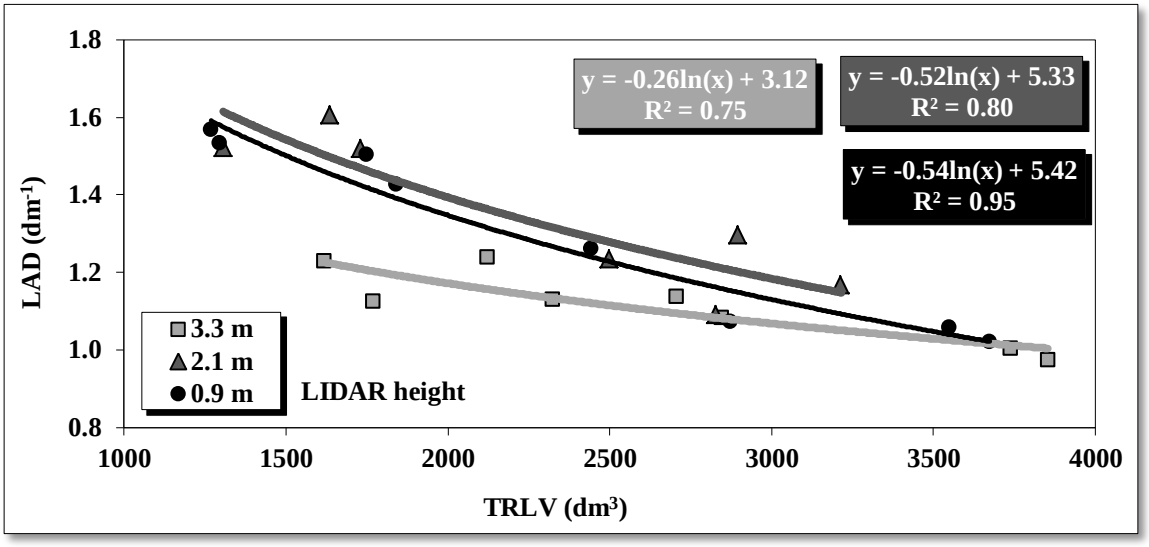

(c)

Fig. 12. Scatter diagram, regression line and R^2 of the relationship between TRLV and LAD of pear-tree blocks. The TRLV was obtained from scans with the sensor placed at three different heights (0.9, 2.1 and 3.3 m) and with two different angular resolutions (1° and 0.5°). **(a)** BI_1, BI_2, BI_3, BI_4, BII_1, BII_2, BII_3, BII_4, $BIII_1$, $BIII_2$, $BIII_3$, $BIII_4$, BIV_1, BIV_2, BIV_3, BIV_4. **(b)** BI_{12}, BI_{34}, BII_{12}, BII_{34}, $BIII_{12}$, $BIII_{34}$, BIV_{12}, BIV_{34}. **(c)** BI_{1234}, BII_{1234}, $BIII_{1234}$, BIV_{1234}. The blocks scanned at different sensor height are shown separately: 0.9 m (black), 2.1m (dark grey) and 3.3 m (light grey).

It can be observed from Fig. 12b that the lowest sensor position (0.9 m) has the best fit with a very high R^2 of 0.93. The worst fit with R^2 =0.58 corresponds to the highest sensor position (3.3 m). With respect to the fitting curves, it can be seen that there is not much difference between the lower (black: 0.9) and intermediate (dark grey: 2.1 m) positions. The trajectory of the fitting curve of the highest position (light grey: 3.3 m) differs from the other two curves and is found below them. The explanation for this is as follows: when the sensor is positioned in the upper part of the vegetation the TRLV obtained are higher and therefore lower LADs are obtained.

The purpose of Fig. 12 as a whole is to show the effect that different blocks lengths have on the relationship between TRLV and LAD.

The results when combining Sections 1-4 of each test, thereby generating four 4 m long blocks (BI_{1234}, BII_{1234}, $BIII_{1234}$, BIV_{1234}), are shown in Fig. 12c. In this case it can be observed that the R^2 for the three heights improves in comparison with Fig. 12b.

The results for sixteen 1 m long blocks are shown in Fig. 12a. In this case it can be observed that the R^2 is lower for the three heights in comparison to Fig. 12b and Fig. 12c. Using smaller sized blocks means that there is greater variability.

Thinking in terms of precision agriculture and future LAD and leaf area estimation studies, it would seem that the appropriate size for blocks in this type of study is a length equal to the distance between trunks (in this particular case 2 m). Though an improved fit was observed when working with 4 m long blocks, the authors of this paper do not consider that the slight improvement observed justifies doubling the block size. On the other hand, there is a clear decrease in the R^2 when working with 1 m long blocks and it seems clear that this block length is taking us away from the most appropriate size.

3.3. Specific study of 2005 for the vine

This study was conducted in the same way as for the pear. Separate analyses were conducted on the effects of the angular resolution and sensor position.

Table 5

Logarithmic regression and R^2 of the relationship between TRLV (x) and LAD (y) of the 8 vine blocks, BI_{12}, BI_{34}, BII_{12}, BII_{34}, $BIII_{12}$, $BIII_{34}$, BIV_{12}, BIV_{34}. The TRLV were obtained from scans with the sensor placed at three different heights (1.2, 1.6 and 2.0 m) and with two different angular resolutions (1° and 0.5°).

Angular resolution	Logarithmic regression	R^2
1°	y= -0.42ln(x)+4.10	0.71
0.5°	y= -0.47ln(x)+4.48	0.76

It was firstly verified whether there was any significant difference when working with angular resolutions of 1° and 0.5° .

Just as happened with the pear tree blocks, the curves of 1° and 0.5° are practically the same in the vine blocks. (Table 5).

Table 6

Regression line and R^2 of the relationship between TRLV (x) and LAD (y) of vine blocks. The TRLV was obtained from scans with the sensor placed at three different heights (1.2, 1.6 and 2.0 m) and with two angular resolutions (1° and 0.5°). The blocks used are: 1m long blocks (BI_1, BI_2, BI_3, BI_4, BII_1, BII_2, BII_3, BII_4, $BIII_1$, $BIII_2$, $BIII_3$, $BIII_4$, BIV_1, BIV_2, BIV_3, BIV_4), 2m long blocks (BI_{12}, BI_{34}, BII_{12}, BII_{34}, $BIII_{12}$, $BIII_{34}$, BIV_{12}, BIV_{34}) and 4m long blocks (BI_{1234}, BII_{1234}, $BIII_{1234}$, BIV_{1234}).

Block length (m)	Number of blocks	Number of data (1°, 0.5°)	Sensor height	Logarithmic regression	R^2
1	16	32	1.2	y= -0.45ln(x)+4.11	0.65
1	16	32	1.6	y= -0.42ln(x)+3.85	0.64

1	16	32	2.0	y= -0.42ln(x)+3.76	0.63
2	8	16	1.2	y= -0.45ln(x)+4.42	0.81
2	8	16	1.6	y= -0.41ln(x)+4.08	0.80
2	8	16	2.0	y= -0.44ln(x)+4.17	0.68
4	4	8	1.2	y= -0.41ln(x)+4.42	0.94
4	4	8	1.6	y= -0.38ln(x)+4.14	0.90
4	4	8	2.0	y= -0.43ln(x)+4.43	0.72

With respect to the sensor height, it can be observed in Table 6 that the highest sensor position (2.0 m) has the worst fit with R^2 values of 0.63, 0.68 and 0.72. The R^2 for the lower (1.2 m) and intermediate (1.6 m) position are practically the same, though a somewhat higher LAD is obtained from the lower position.

The main purpose of Table 6 is to show the effect that different blocks lengths have on the relationship between TRLV and LAD.

In the case of 4 m long blocks it can be observed that the R^2 for the three heights improves in comparison with 2 m long blocks with an R^2 of 0.94 being obtained when the sensor is placed at a height of 1.2 m (Table 6).

In the case of 1 m long blocks it can be observed that the R^2 is lower for the three heights in comparison to 2 m long blocks and 4 m long blocks. Using smaller sized blocks means that there is greater variability.

Thinking in terms of precision agriculture and future LAD and leaf area estimation studies, it would seem that the appropriate size for blocks in this type of study is a length equal to the distance between trunks (in this particular case 2 m). An improved fit was observed when working with 4 m long blocks and the authors of this paper do not dismiss the possibility of working with this block length. While it is true that the size of the vegetation to be defoliated is doubled, vines are not normally as large as fruit trees and the extra work required for defoliation is relatively little.

4. Conclusions

The TRLV of the crops with hedgerow configuration which were studied in this paper, — apple trees (*M. communis* L. 'Red Chief' and 'Golden'), pear trees (*P. communis* L. 'Conference' and 'Blanquilla') and vines (*V. vinifera* L. 'Cabernet Sauvignon' and 'Merlot') —, appears in itself to explain the LAD. Competition of the leaves for light and the occupation of volume/space by the leaves seem to follow a similar model in the three crops. At plant level and without taking into account the vertical divisions, a good logarithmic fit is found, $y = -0.36 \ln(x) + 3.69$ with $R^2=0.87$ between TRLV (x) in dm^3 and LAD (y) in dm^{-1}. This result confirms the initial hypothesis that predicted the existence of a non-linear relationship between the TRLV and the LAD. For reasons intrinsically related to the plant and the procedure, in the uppermost section/stratum a different relationship between TRLV and LAD was obtained in comparison to the rest of the plant. However, its influence on the block of vegetation as a whole is small. The lowest stratum (area of the

626 trunk) also has little influence on the block as a whole due to the small amount of
627 vegetation. The LAD can be estimated from the TRLV. If the LAD is multiplied by the
628 TRLV, the leaf area of the vegetation under study can be also estimated. It is therefore
629 concluded that by using the information provided by the LIDAR 3D Dynamic
630 Measurement System, a good estimation can be obtained of the leaf area in hedgerow fruit
631 tree crops and hedgerow vineyards. No differences were observed between using the
632 LIDAR with angular resolutions of 1º or 0.5º when estimating the LAD. The LIDAR height
633 position affects LAD estimation. The lowest of the three tested positions gives the highest
634 R^2 and, therefore, the best correlation between TRLV and LAD. The use, in future tests, of
635 block lengths equal to the distance between trunks would appear to the appropriate method
636 to follow.
637
638
639 **Acknowledgements**
640
641 This work has been funded by the Spanish Ministry of Science and Innovation and by the
642 European Union through the FEDER funds and is part of research projects Pulvexact
643 (AGL2002-04260-C04-02), Optidosa (AGL2007-66093-C04-03) and Safespray
644 (AGL2010-22304-C04-03).
645
646
647 **References**
648

649 Chen, J. and Black, T., 1992. Defining leaf-area index for non-flat leaves. Plant Cell
650 Environment. 15, 421-429.

651 Cohen, S., Raveh, E., Li, Y., Grava, A., Goldschmidt, E., 2005. Physiological responses of
652 leaves, tree growth and fruit yield of grapefruit trees under reflective shade screens.
653 Sci. Hortic. 107, 25-35.

654 Dworak, V., Selbeck, J., Ehlert, D., 2011. Ranging sensors for vehicle-based measurement
655 of crop stand and orchard parameters: a review. Trans. ASABE. 54, 1497-1510.

656 Goodwin, I., Whitfield, D., Connor, D., 2006. Effects of tree size on water use of peach
657 (Prunus persica L. Batsch). Irrigation Sci. 24, 59-68.

658 Keightley, K.E., Bawden, G.W., 2010. 3D volumetric modeling of grapevine biomass using
659 Tripod LiDAR. Comput. Electron. Agric. 74, 305-312.

660 Lee, K.H., Ehsani, R., 2009. A laser scanner based measurement system for quantification
661 of citrus tree geometric characteristics. Appl. Eng. Agric. 25, 777-788.

662 Llorens, J., Gil, E., Llop, J., Escola, A., 2011a. Ultrasonic and LIDAR sensors for
663 electronic canopy characterization in vineyards: advances to improve pesticide
664 application methods. sensors. 11, 2177-2194.

665 Llorens, J., Gil, E., Llop, J., Queralto, M., 2011b. Georeferenced LiDAR 3D vine
666 plantation map generation. Sensors. 11, 6237-6256.

667 Lopez-Lozano, R., Baret, F., Lebon, E., Tisseyre, B., 2011. 2D approximation of realistic
668 3D vineyard row canopy representation for light interception (fIPAR) and light
669 intensity distribution on leaves (LIDIL). Eur. J. Agron. 35, 171-183.

670 Moorthy, I., Miller, J., Jimenez, Berni, J., Zarco Tejada, P., Hu, B., Chen, J., 2011. Field
671 characterization of olive (Olea europaea L.) tree crown architecture using terrestrial
672 laser scanning data. Agric. For. Meteorol. 151, 204-214.

673 Orgaz, F., Testi, L., Villalobos, F., Fereres, E., 2006. Water requirements of olive orchards
674 - II: Determination of crop coefficients for irrigation scheduling. Irrigation. Sci. 24, 77-
675 84.

676 Palacin, J., Palleja, T., Tresanch, M., Sanz, R., Llorens, J., Ribes-Dasi, M., Masip, J., Arnó,
677 J., Escolà, A., Rosell, J.R., 2007. Real-time tree-foliage surface estimation using a
678 ground laser scanner. IEEE Trans. Instrum. Meas. 56, 1377-1383.

679 Palleja, T., Tresanchez, M., Teixido, M., Sanz, R., Rosell, J.R., Palacin, J., 2010.
680 Sensitivity of tree volume measurement to trajectory errors from a terrestrial LIDAR
681 scanner. Agric. For. Meteorol. 150, 1420-1427.

682 Pascual, M., Villar, J.M., Rufat, J., Rosell, J.R., Sanz, R., Arno, J., 2011. Evaluation of
683 peach tree growth characteristics under different irrigation strategies by LIDAR
684 system: preliminary results. Acta Hortic. 889, 227-232.

685 Pereira, A., Green, S., 2007. Sap flow, leaf area, net radiation and the Priestley-Taylor
686 formula for irrigated orchards and isolated trees. Agric. Water Manage. 92, 48-52.

687 Pereira, A., Green, S., Villa Nova N., 2007. Relationships between single tree canopy and
688 grass net radiations. Agric. For. Meteorol. 142, 45-49.

689 Rosell, J., Sanz, R., Llorens, J., Arno, J., Escolà, A., Ribes-Dasi, M., Masip, J., Camp, F.,
690 Gràcia, F., Solanelles, F., Pallejà, T., Val, L., Planas, S., Gil, E., Palacín, J., 2009a. A
691 tractor-mounted scanning LIDAR for the non-destructive measurement of vegetative
692 volume and surface area of tree-row plantations: a comparison with conventional
693 destructive measurements. Biosys. Eng. 102, 128-134.

694 Rosell, J., Llorens, J., Sanz, R., Arno, J., Ribes-Dasi, M., Masip, J., Escolà, A., Camp, F.,
695 Solanelles, F., Gràcia, F., Gil, E., Val, L., Planas, S., Palacín, J., 2009b. Obtaining the
696 three-dimensional structure of tree orchards from remote 2D terrestrial LIDAR
697 scanning. Agric. For. Meteorol. 149, 1505-1515.

698 Rosell, J., Sanz, R., 2012. A review of methods and applications of the geometric
699 characterization of tree crops in agricultural activities. Comput. Electron. Agric. 81,
700 124-141.

701 Sanz-Cortiella, R., Llorens-Calveras, J., Rosell-Polo, J.R., Gregorio-Lopez, E., Palacin-
702 Roca, J., 2011a. Characterisation of the LMS200 Laser Beam under the influence of
703 blockage surfaces. Influence on 3D scanning of tree orchards. Sensors. 11, 2751-2772.

704 Sanz-Cortiella, R., Llorens-Calveras, J., Escola, A., Arno-Satorra, J., Ribes-Dasi, M.,
705 Masip-Vilalta, J., Camp, F., Gracia-Aguila, F., Solanelles-Batlle, F., Planas-DeMarti,
706 S., Pallejà-Cabré, T., Palacín-Roca, J., Gregorio-Lopez, E., Del-Moral-Martínez, I.,
707 Rosell-Polo, J.R., 2011b. Innovative LIDAR 3D dynamic measurement system to
708 estimate fruit-tree leaf area. Sensors. 11, 5769-5791.

709 Testi, L., Villalobos, F., Orgaz, F., 2004. Evapotranspiration of a young irrigated olive
710 orchard in southern Spain. Agric. For. Meteorol. 121, 1-18.

711 Walklate, P., 1989. A laser scanning instrument for measuring crop geometry. Agric. For.
712 Meteorol. 46, 275-284.

713 Walklate, P., Richardson, G., Baker, D., Richards, P., Cross, J., 1997. Short-range LIDAR
714 measurement of top fruit tree canopies for pesticide applications research in the UK.
715 Advances in Laser Remote Sensing for Terrestrial and Oceanographic Applications.
716 Vol. 3059, pp. 143-151.

717 Walklate, P., Cross, J., Richardson, G., Murray, R., Baker, D., 2002. Comparison of
718 different spray volume deposition models using LIDAR measurements of apple
719 orchards. Biosyst. Eng. 82, 253-267.

720 Wei, J., Salyani, M., 2004. Development of a laser scanner for measuring tree canopy
721 characteristics: phase 1. Prototype development. Trans. ASAE. 47, 2101-2107.

722 Wei, J., Salyani, M., 2005. Development of a laser scanner for measuring tree canopy
723 characteristics: phase 2. Foliage density measurement. Trans. ASAE. 48, 1595-1601.

724 Williams, L., Ayars, J., 2005. Grapevine water use and the crop coefficient are linear
725 functions of the shaded area measured beneath the canopy. Agric. For. Meteorol. 132,
726 201-211.

727 Zheng, G., Moskal, L.M., 2009. Retrieving leaf area index (LAI) using remote sensing:
728 Theories, methods and sensors. Sensors. 9, 2719-2745.

729
730